Trajectory Optimization Framework for Rehabilitation Robots - Supplementary Material

Model

Author(s):
Sommerhalder, Michael; Zimmermann, Yves; Simovic, Leonardo; Hutter, Marco; Wolf, Peter; Riener, Robert

Publication date:
2023-05-23

Permanent link:
https://doi.org/10.3929/ethz-b-000612984

Trajectory Optimization Framework for Rehabilitation Robots with Multi-Workspace Objectives and Constraints Supplementary Material

Michael Sommerhalder[*,1] and Yves Zimmermann[*,1,2], Leonardo Simovic[1], Marco Hutter[2], Peter Wolf[1], Robert Riener[1,3]

I. Hybrid Differentiation

To calculate the higher-order derivatives of the parameterization, a linear combination between forward and backward finite difference coefficients c of precision 2 was applied [?]. The forward coefficients are:

$$\begin{aligned} \boldsymbol{c}_{F0} &= \{1\} \\ \boldsymbol{c}_{F1} &= \{-1.5, 2, -0.5\} \\ \boldsymbol{c}_{F2} &= \{2, -5, 4, -1\} \\ \boldsymbol{c}_{F3} &= \{-2.5, 9, -12, 7, -1.5\} \end{aligned} \tag{1}$$

And the backward coefficients:

$$\begin{aligned} \boldsymbol{c}_{B0} &= \{1\} \\ \boldsymbol{c}_{B1} &= \{0.5, -2, 1.5\} \\ \boldsymbol{c}_{B2} &= \{-1, 4, -5, 2\} \\ \boldsymbol{c}_{B3} &= \{1.5, -7, 12, -9, 2.5\} \end{aligned} \tag{2}$$

The hybrid differentiation function results in:

$$\begin{aligned} \left(\frac{\delta^j \boldsymbol{q}}{\delta t^j}\right)_k &= f_j(\boldsymbol{q}_{k-j-1}, \dots, \boldsymbol{q}_{k+j+1}) \\ &= \begin{cases} A, & \text{if } k < j+1 \\ B, & \text{if } k > N-j-1 \\ \alpha A + \beta B, & \text{else} \end{cases} \\ \beta &= \frac{k-j-1}{N-2j-2}, \quad \alpha = 1-\beta \\ A &= \boldsymbol{c}_{Fj}[\boldsymbol{q}_k, \dots, \boldsymbol{q}_{k+j+1}]^T \\ B &= \boldsymbol{c}_{Bj}[\boldsymbol{q}_{k-j-1}, \dots, \boldsymbol{q}_k]^T \end{aligned} \tag{3}$$

The parameterization derivative can also be expressed in dense form with matrix D_j, containing the corresponding forward and backward coefficients as elements.

II. CJC to HND Transformation ($^{\text{HND}}_{\text{CJC}}\chi$)

The transformation from CJC and HND can be calculated via forward kinematics. In the following, these abbreviations are used for rotations in 3D-space:

$$\begin{aligned} \boldsymbol{R}_x(\theta) &:= \begin{pmatrix} 1 & 0 & 0 \\ 0 & \cos(\theta) & -\sin(\theta) \\ 0 & \sin(\theta) & \cos(\theta) \end{pmatrix} \\ \boldsymbol{R}_y(\theta) &:= \begin{pmatrix} \cos(\theta) & 0 & \sin(\theta) \\ 0 & 1 & 0 \\ -\sin(\theta) & 0 & \cos(\theta) \end{pmatrix} \\ \boldsymbol{R}_z(\theta) &:= \begin{pmatrix} \cos(\theta) & -\sin(\theta) & 0 \\ \sin(\theta) & \cos(\theta) & 0 \\ 0 & 0 & 1 \end{pmatrix} \end{aligned} \tag{4}$$

The rotation from the torso fixed system to the hand can be calculated as a series of consecutive rotations:

$$\begin{aligned} \boldsymbol{R}_{\text{POE}} &= \boldsymbol{R}_z(q_{\text{POE}}) \\ \boldsymbol{R}_{\text{AOE}} &= \boldsymbol{R}_{\text{POE}}\boldsymbol{R}_y(-\frac{\pi}{2})\boldsymbol{R}_z(q_{\text{AOE}}) \\ \boldsymbol{R}_{\text{IER}} &= \boldsymbol{R}_{\text{AOE}}\boldsymbol{R}_y(-\frac{\pi}{2})\boldsymbol{R}_z(q_{\text{IER}}) \\ \boldsymbol{R}_{\text{EFE}} &= \boldsymbol{R}_{\text{IER}}\boldsymbol{R}_y(-\frac{\pi}{2})\boldsymbol{R}_x(-\frac{\pi}{2})\boldsymbol{R}_z(q_{\text{EFE}}) \\ \boldsymbol{R}_{\text{WPS}} &= \boldsymbol{R}_{\text{EFE}}\boldsymbol{R}_y(\frac{\pi}{2})\boldsymbol{R}_z(q_{\text{WPS}}) \\ \boldsymbol{R}_{\text{WFE}} &= \boldsymbol{R}_{\text{WPS}}\boldsymbol{R}_x(\frac{\pi}{2})\boldsymbol{R}_z(q_{\text{WFE}}) \\ \boldsymbol{R}_{\text{WUR}} &= \boldsymbol{R}_{\text{WFE}}\boldsymbol{R}_y(-\frac{\pi}{2})\boldsymbol{R}_z(q_{\text{WUR}}) \\ \boldsymbol{R}_{\text{HND}} &= \boldsymbol{R}_{\text{WUR}}\boldsymbol{R}_x(\pi)\boldsymbol{R}_z(-\frac{\pi}{2}) \end{aligned} \tag{5}$$

And the corresponding hand coordinates w.r.t. the glenohumeral joint in world coordinates:

$$\begin{aligned} \boldsymbol{p}_{\text{UA}} &= \boldsymbol{R}_{\text{IER}} \begin{pmatrix} 0 \\ 0 \\ l_{\text{UA}} \end{pmatrix} \\ \boldsymbol{p}_{\text{FA}} &= \boldsymbol{p}_{\text{UA}} + \boldsymbol{R}_{\text{EFE}} \begin{pmatrix} l_{\text{FA}} \\ 0 \\ 0 \end{pmatrix} \\ \boldsymbol{p}_{\text{HND}} &= \boldsymbol{p}_{\text{FA}} + \boldsymbol{R}_{\text{WUR}} \begin{pmatrix} 0 \\ \frac{l_{\text{WR}}}{2} \\ 0 \end{pmatrix} \end{aligned} \tag{6}$$

Here, l_{UA} is the upper arm length, l_{FA} is the forearm length and l_{WR} is the wrist length of the patient. Further, the elbow

*The first two authors contributed equally to this paper.

[1] The author is with Sensory-Motor Systems Lab, ETH Zurich, Switzerland. somichae@ethz.ch

[2] The author is with Robotic Systems Lab, ETH Zurich, Switzerland.

[3] The author is with Spinal Cord Injury Center, University Hospital Balgrist, Zurich, Switzerland. rriener@ethz.ch

This research was supported in part by Innosuisse, the Swiss Innovation Agency, ID 33759.1 IP-LS.

swivel angle ϕ is calculated as follows:

$$
\begin{aligned}
r &= \frac{1}{1+e^{-1000(\alpha-0.01)}}, \quad \alpha = 1-\frac{|\boldsymbol{u}_z \cdot \boldsymbol{p}_{\text{HND}}|}{||\boldsymbol{p}_{\text{HND}}||} \\
\boldsymbol{n} &= r\left(\boldsymbol{u}_z \times \boldsymbol{p}_{\text{HND}}\right)+(1-r)\,\boldsymbol{u}_x \\
\phi &= \operatorname{acos}\left(\frac{\boldsymbol{n}\cdot(\boldsymbol{R}_{\text{EFE}}\boldsymbol{u}_z)}{||\boldsymbol{n}||\cdot||\boldsymbol{R}_{\text{EFE}}\boldsymbol{u}_z||}\right),
\end{aligned} \tag{7}
$$

where r estimates the elbow condition to prevent singularities when the arm is fully extended. $\boldsymbol{u}_x$ and $\boldsymbol{u}_z$ are unit vectors in x and z direction respectively. The final HND coordinates result in:

$$
\begin{pmatrix}
p_{\text{HND},x} \\ p_{\text{HND},y} \\ p_{\text{HND},z} \\ \phi \\ Q(\boldsymbol{R}_{\text{HND}})_w \\ Q(\boldsymbol{R}_{\text{HND}})_x \\ Q(\boldsymbol{R}_{\text{HND}})_y \\ Q(\boldsymbol{R}_{\text{HND}})_z
\end{pmatrix} \tag{8}
$$

with Q being the conversion from rotation matrix to quaternion.

III. HND to CJC Transformation ($^{\text{CJC}}_{\text{HND}}\chi$)

The normal vector of the elbow triangle $\boldsymbol{n}$ can be determined by the following system of equations

$$
\begin{cases}
\boldsymbol{n}\cdot \boldsymbol{z}_n = cos(\theta), \\
\boldsymbol{n}\cdot \boldsymbol{p}_{\text{FA}} = 0, \\
||\boldsymbol{n}|| = 1
\end{cases} \tag{9}
$$

which, when solving analytically, yields two solutions $\boldsymbol{n}_1$ and $\boldsymbol{n}_2$ for a possible positive and negative θ:

$$
\begin{aligned}
a &= \frac{\boldsymbol{p}_{\text{FA,y}}\boldsymbol{z}_{n,z}-\boldsymbol{p}_{\text{FA,z}}\boldsymbol{z}_{n,y}}{\boldsymbol{p}_{\text{FA,x}}\boldsymbol{z}_{n,y}-\boldsymbol{p}_{\text{FA,y}}\boldsymbol{z}_{n,x}} \\
b &= \frac{-cos(\theta)\boldsymbol{p}_{\text{FA,y}}}{\boldsymbol{p}_{\text{FA,x}}\boldsymbol{z}_{n,y}-\boldsymbol{p}_{\text{FA,y}}\boldsymbol{z}_{n,x}} \\
c &= \frac{\boldsymbol{p}_{\text{FA,z}}\boldsymbol{z}_{n,x}-\boldsymbol{p}_{\text{FA,x}}\boldsymbol{z}_{n,z}}{\boldsymbol{p}_{\text{FA,x}}\boldsymbol{z}_{n,y}-\boldsymbol{p}_{\text{FA,y}}\boldsymbol{z}_{n,x}} \\
d &= \frac{cos(\theta)\boldsymbol{p}_{\text{FA,x}}}{\boldsymbol{p}_{\text{FA,x}}\boldsymbol{z}_{n,y}-\boldsymbol{p}_{\text{FA,y}}\boldsymbol{z}_{n,x}} \\
e &= \sqrt{c^2\left(1+c^2-d^2-b^2\left(c^2+1\right)\right)} \\
\boldsymbol{n}_{1,x} &= b, \quad \boldsymbol{n}_{1,y} = \frac{d-e}{c^2+1}, \quad \boldsymbol{n}_{1,z} = -\frac{e+c^2d}{c^3+c} \\
\boldsymbol{n}_{2,x} &= b, \quad \boldsymbol{n}_{2,y} = \frac{d+e}{c^2+1}, \quad \boldsymbol{n}_{2,z} = \frac{e-c^2d}{c^3+c}
\end{aligned} \tag{10}
$$

Further, the upper arm position $\boldsymbol{p}_{\text{UA}}$ can be found:

$$
\begin{aligned}
r &= \frac{\boldsymbol{n}\times\boldsymbol{p}_{\text{FA}}}{||\boldsymbol{n}\times\boldsymbol{p}_{\text{FA}}||}\cdot\frac{\sqrt{s\left(s-l_{\text{FA}}\right)\left(s-l_{\text{UA}}\right)\left(s-||\boldsymbol{p}_{\text{FA}}||\right)}}{2||\boldsymbol{p}_{\text{FA}}||}, \\
h &= \frac{\boldsymbol{p}_{\text{FA}}}{||\boldsymbol{p}_{\text{FA}}||}\cdot\frac{\sqrt{s\left(s-l_{\text{FA}}\right)\left(s-l_{\text{UA}}\right)\left(s-||\boldsymbol{p}_{\text{FA}}||\right)}}{2||\boldsymbol{p}_{\text{FA}}||\cdot\tan\left(\operatorname{acos}\left(\frac{l_{\text{UA}}^2+||\boldsymbol{p}_{\text{FA}}||^2-l_{\text{FA}}^2}{2l_{\text{UA}}||\boldsymbol{p}_{\text{FA}}||}\right)\right)}, \\
\boldsymbol{p}_{\text{UA}} &= r+h
\end{aligned} \tag{11}
$$

Having the elbow position, the first two clinical joints can be determined:

$$
\begin{aligned}
q_{\text{POE}} &= \operatorname{atan2}\left(\left(\frac{\boldsymbol{p}_{\text{UA}}}{l_{\text{UA}}}\right)_y, \left(\frac{\boldsymbol{p}_{\text{UA}}}{l_{\text{UA}}}\right)_x\right) \\
q_{\text{AOE}} &= \operatorname{acos}\left(-\frac{\boldsymbol{p}_{\text{UA}}}{l_{\text{UA}}}\cdot\boldsymbol{e}_z\right)
\end{aligned} \tag{12}
$$

The rotation from the torso fixed system to the AOE frame $\boldsymbol{R}_{\text{AOE}}$ can be calculated as seen in eq. (5). Next, the third and fourth clinical joints can be determined:

$$
\begin{aligned}
\boldsymbol{u} &= \boldsymbol{R}_{\text{AOE}}^T\boldsymbol{p}_{\text{FA}} \\
q_{\text{IER}} &= \operatorname{atan2}\left(\boldsymbol{u}_z, \boldsymbol{u}_y\right) \\
q_{\text{EFE}} &= \operatorname{acos}\left(\frac{l_{\text{FA}}^2+l_{\text{UA}}^2-||\mathbf{p}_{\text{FA}}||^2}{2l_{\text{FA}}l_{\text{UA}}}\right)-\pi
\end{aligned} \tag{13}
$$

The wrist joints can be determined by finding the Euler ZYX coordinates from the resulting rotation matrix:

$$
R_D = \mathbf{R}_{\text{EFE}}^T\mathbf{R}_{\text{WUR}} \tag{14}
$$

IV. Comparison between different arm lengths

This additional experiment investigated the adaptation of generated trajectories to different arm lengths (see Fig. 1). The reference trajectory was taken from Subject 5 from the U-Limb dataset (upper-arm length $l_{\text{UA}} = 0.32$m, forearm length $l_{\text{FA}} = 0.27$m, wrist joint to center length $l_{\text{WR}} = 0.035$m). The Subjects with the longest and shortest arm lengths were chosen as comparatives. Subject 40 had the longest ($l_{\text{UA}} = 0.38$m, $l_{\text{FA}} = 0.29$m, $l_{\text{WR}} = 0.03$m) and Subject 19 the shortest ($l_{\text{UA}} = 0.24$m, $l_{\text{FA}} = 0.20$m, $l_{\text{WR}} = 0.025$m) lengths. Thereby, for the sake of consistency (e.g., generation within a sequence of movements), start and goal positions in HND space were constrained. The reference trajectory and jerk were optimized for the individual arm lengths.

Results showed that the bookshelf was moved closer for the patient with a shorter arm length ($x = 0.40$m at $t = 4.5$s) and moved further away for the patient with a larger arm length ($x = 0.59$m at $t = 4.5$s) (see Fig. 1, position, HND, X). Similarly, the bookshelf was placed higher for Subject 40 ($z = 0.20$m at $t = 5$s) than for Subject 19 ($z = 0.14$m at $t = 5$s). Although the task changed in HND space, the resulting trajectory in the clinical space stayed almost identical for all Subjects (see Fig. 1, position, CJC). Since the significantly shorter upper- and forearm lengths of patient 2 did not allow to reach the required initial position, the generator optimized for the closest position with a fully extended elbow (see Fig. 1, position CJC, EFE). These results demonstrate that our framework could preserve the initial shape of a learned LbD trajectory while adapting the task to the individual arm lengths of new patients.

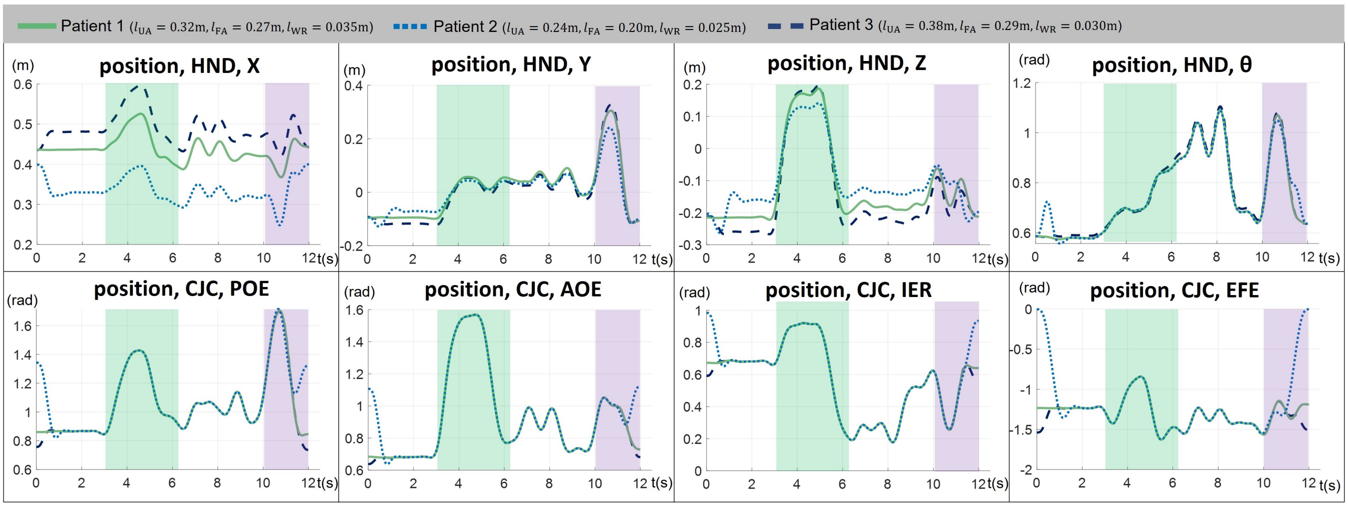

Fig. 1. Comparison of a generated 'Reach and grasp a book' trajectory for three patients of the U-Limb dataset with different anthropometries (Patient 1: Subject 5. Patient 2: Subject 19. Patient 3: Subject 40). The reference trajectory was taken from Patient 1. Start and goal constraints were defined in HND space. The upper- and forearm lengths of patient 2 did not allow to reach the required initial x position. As a consequence, the generator optimized for the closest position with a fully extended elbow (see start and goal position CJC, EFE).